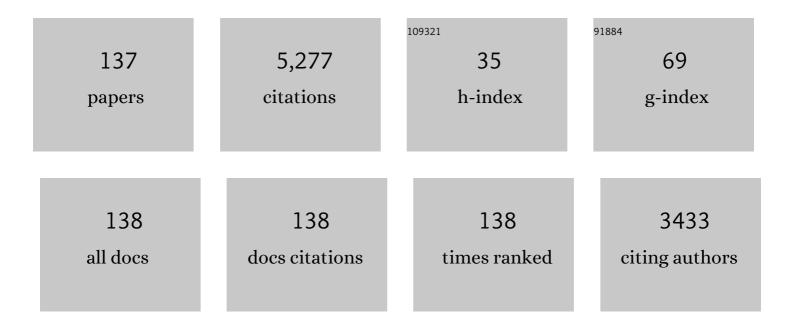
List of Publications by Year in descending order

Source: https://exaly.com/author-pdf/3736591/publications.pdf Version: 2024-02-01



#	Article	IF	CITATIONS
1	Visible-Wavelength All-Fiber Mode-Locked Vortex Laser. Journal of Lightwave Technology, 2022, 40, 191-195.	4.6	13
2	Towards Power Scaling of Simple CW Ultraviolet via Pr: LiYF ₄ -LBO Laser at 320 nm. IEEE Photonics Technology Letters, 2022, 34, 129-132.	2.5	8
3	Tunable, Continuous-Wave, Deep-Ultraviolet Laser Generation by Intracavity Frequency Doubling of Visible Fiber Lasers. Journal of Lightwave Technology, 2022, 40, 3900-3906.	4.6	4
4	Visibleâ€Wavelength Spatiotemporal Mode‣ocked Fiber Laser Delivering 9 ps, 4 nJ Pulses at 635 nm. Laser and Photonics Reviews, 2022, 16, .	8.7	27
5	On-chip mid-IR octave-tunable Raman soliton laser. Optics Express, 2022, 30, 25356.	3.4	1
6	Ultra‧mall 2D PbS Nanoplatelets: Liquidâ€Phase Exfoliation and Emerging Applications for Photoâ€Electrochemical Photodetectors. Small, 2021, 17, e2005913.	10.0	50
7	Direct generation of watt-level yellow Dy ³⁺ -doped fiber laser. Photonics Research, 2021, 9, 446.	7.0	55
8	3ÂW average-power high-order mode pulse in dissipative soliton resonance mode-locked fiber laser. Nanophotonics, 2021, 10, 3527-3539.	6.0	10
9	Visible-Wavelength-Tunable, Vortex-Beam Fiber Laser Based on a Long-Period Fiber Grating. IEEE Photonics Technology Letters, 2021, 33, 1173-1176.	2.5	4
10	Externally Pumped Photonic Chipâ€Based Ultrafast Raman Soliton Source. Laser and Photonics Reviews, 2021, 15, 2000301.	8.7	11
11	Intracavity Frequency Doubling Deep-Ultraviolet Ho3+: ZBLAN Fiber Laser with Wavelength Tuning from 269.5 to 275.4 nm. , 2021, , .		0
12	A few-layer InSe-based sensitivity-enhanced photothermal fiber sensor. Journal of Materials Chemistry C, 2020, 8, 132-138.	5.5	15
13	919.8Ânm self-Q-switched Nd-doped silica all-fiber laser. Optics Communications, 2020, 473, 125939.	2.1	3
14	MXene Ti ₃ C ₂ T _x saturable absorber for passively Q-switched mid-infrared laser operation of femtosecond-laser–inscribed Er:Y ₂ O ₃ ceramic channel waveguide. Nanophotonics, 2020, 9, 2495-2503.	6.0	29
15	Graphdiyneâ€Polymer Nanocomposite as a Broadband and Robust Saturable Absorber for Ultrafast Photonics. Laser and Photonics Reviews, 2020, 14, 1900367.	8.7	99
16	Visible-light all-fiber vortex lasers based on mode selective couplers*. Chinese Physics B, 2020, 29, 094204.	1.4	4
17	A self-powered photodetector based on two-dimensional boron nanosheets. Nanoscale, 2020, 12, 5313-5323.	5.6	60
18	Towards visible-wavelength passively mode-locked lasers in all-fibre format. Light: Science and Applications, 2020, 9, 61.	16.6	52

#	Article	IF	CITATIONS
19	Real-time observation of vortex mode switching in a narrow-linewidth mode-locked fiber laser. Photonics Research, 2020, 8, 1203.	7.0	22
20	Visible-wavelength pulsed lasers with low-dimensional saturable absorbers. Nanophotonics, 2020, 9, 2273-2294.	6.0	20
21	Mid-infrared all-fiber gain-switched pulsed laser at 3 μm. Opto-Electronic Advances, 2020, 3, 190032-190032.	13.3	11
22	Novel Optical and Photonic Devices based on 2D Materials: feature issue introduction. Optical Materials Express, 2020, 10, 1344.	3.0	0
23	What makes the best chip-scale photonic sensor?. , 2020, , .		Ο
24	On-chip supercontinuum generation in Ge28Sb12Se60 chalcogenide waveguides and numerical investigation. , 2020, , .		0
25	Green/red pulsed vortex-beam oscillations in all-fiber lasers with visible-resonance gold nanorods. Nanoscale, 2019, 11, 15991-16000.	5.6	19
26	Intra-Cavity Mode-Selective Coupler Assisted Ultrafast Cylindrical Vector Fiber Laser. , 2019, , .		0
27	High-Order Vortex Generation From CW and Passively Q-Switched Pr:YLF Visible Lasers. IEEE Photonics Technology Letters, 2019, 31, 1457-1460.	2.5	20
28	Visible-Wavelength All-Fiber Vortex Laser. IEEE Photonics Technology Letters, 2019, 31, 1487-1490.	2.5	9
29	Optimizing the Self-Amplitude Modulation of Different 2-D Saturable Absorbers for Ultrafast Mode-Locked Fiber Lasers. IEEE Journal of Selected Topics in Quantum Electronics, 2019, 25, 1-10.	2.9	6
30	Unveiling the Stimulated Robust Carrier Lifetime of Surfaceâ€Bound Excitons and Their Photoresponse in InSe. Advanced Materials Interfaces, 2019, 6, 1900171.	3.7	18
31	Ultrafast Raman Fiber Laser Based on Cavity Matching Scheme and Heavily Germania-Core Fiber. Journal of Lightwave Technology, 2019, 37, 2914-2919.	4.6	5
32	Sub-15-ns Passively Q-Switched Er:YSGG Laser at <inline-formula> <tex-math notation="LaTeX">\$2.8~mu\$ </tex-math </inline-formula> m With Fe:ZnSe Saturable Absorber. IEEE Photonics Technology Letters, 2019, 31, 565-568.	2.5	14
33	2.01–2.42 <inline-formula> <tex-math notation="LaTeX">\$mu\$</tex-math> </inline-formula> m All-Fiber Femtosecond Raman Soliton Generation in a Heavily Germanium Doped Fiber. IEEE Journal of Selected Topics in Quantum Electronics, 2019, 25, 1-7.	2.9	18
34	Ultrathin GeSe Nanosheets: From Systematic Synthesis to Studies of Carrier Dynamics and Applications for a High-Performance UV–Vis Photodetector. ACS Applied Materials & Interfaces, 2019, 11, 4278-4287.	8.0	105
35	Determining topological charge based on an improved Fizeau interferometer. Optics Express, 2019, 27, 12774.	3.4	41
36	Compact all-fiber 21-27 <i>î¼</i> m tunable Raman soliton source based on germania-core fiber. Optics Express, 2019, 27, 28544.	3.4	19

#	Article	IF	CITATIONS
37	2166 nm all-fiber short-pulsed Raman laser based on germania-core fiber. Optics Express, 2019, 27, 34552.	3.4	6
38	High-efficiency, yellow-light Dy ³⁺ -doped fiber laser with wavelength tuning from 5687 to 5819  nm. Optics Letters, 2019, 44, 4423.	3.3	30
39	Direct generation of orthogonally polarized dual-wavelength continuous-wave and passively Q-switched vortex beam in diode-pumped Pr:YLF lasers. Optics Letters, 2019, 44, 5586.	3.3	11
40	Visible Raman and Brillouin lasers from a microresonator/ZBLAN-fiber hybrid system. Photonics Research, 2019, 7, 566.	7.0	9
41	Direct generation of an ultrafast vortex beam in a CVD-graphene-based passively mode-locked Pr:LiYF ₄ visible laser. Photonics Research, 2019, 7, 1209.	7.0	36
42	Cascaded Brillouin, Raman, and Four-Wave-Mixing Generation in a 1.06-μm Microsphere-Feedback Yb-Fiber Laser. IEEE Photonics Journal, 2018, 10, 1-8.	2.0	1
43	2 Âμm high-power dissipative soliton resonance in a compact Ϊƒ-shaped Tm-doped double-clad fiber laser. Applied Physics Express, 2018, 11, 052701.	2.4	41
44	Efficient continuous-wave and short-pulse Ho ³⁺ -doped fluorozirconate glass all-fiber lasers operating in the visible spectral range. Nanoscale, 2018, 10, 5272-5279.	5.6	36
45	Bidirectional Red-Light Passively Q-Switched All-Fiber Ring Lasers With Carbon Nanotube Saturable Absorber. Journal of Lightwave Technology, 2018, 36, 2694-2701.	4.6	23
46	Effects of Nanomaterial Saturable Absorption on Passively Mode-Locked Fiber Lasers in an Anomalous Dispersion Regime: Simulations and Experiments. IEEE Journal of Selected Topics in Quantum Electronics, 2018, 24, 1-9.	2.9	9
47	Passively Mode-Locked Tm3+-Doped Fiber Laser With Gigahertz Fundamental Repetition Rate. IEEE Journal of Selected Topics in Quantum Electronics, 2018, 24, 1-6.	2.9	38
48	Effects of nanomaterial saturable absorption on gain-guide soliton in a positive group-dispersion fiber laser: Simulations and experiments. Optics Communications, 2018, 406, 163-168.	2.1	1
49	Miniaturized Mid-Infrared All-Fiber Laser Passively Q-Switched by Topological Insulator Bi <inf>2</inf> Se <inf>3</inf> ., 2018, , .		2
50	Self-Q-switched and wavelength-tunable tungsten disulfide-based passively Q-switched Er:Y ₂ O ₃ ceramic lasers. Photonics Research, 2018, 6, 830.	7.0	30
51	1.7-\$mu\$m Tm/Ho-Codoped All-Fiber Pulsed Laser Based on Intermode-Beating Modulation Technique. Journal of Lightwave Technology, 2018, 36, 4894-4899.	4.6	16
52	Incorporating MoS ₂ saturable absorption with nonlinear polarization rotation for stabilized mode-locking fibre lasers. Laser Physics Letters, 2018, 15, 075102.	1.4	16
53	High-order mode direct oscillation of few-mode fiber laser for high-quality cylindrical vector beams. Optics Express, 2018, 26, 11850.	3.4	56
54	Chip-scale broadband spectroscopic chemical sensing using an integrated supercontinuum source in a chalcogenide glass waveguide. Photonics Research, 2018, 6, 506.	7.0	78

ZHENGQIAN LUO

#	Article	IF	CITATIONS
55	Ultrawide-Space and Controllable Soliton Molecules in a Narrow-Linewidth Mode-Locked Fiber Laser. IEEE Photonics Technology Letters, 2018, 30, 1423-1426.	2.5	10
56	Compact self-Q-switched, tunable mid-infrared all-fiber pulsed laser. Optics Express, 2018, 26, 34497.	3.4	12
57	Dynamic mode-switchable optical vortex beams using acousto-optic mode converter. Optics Letters, 2018, 43, 5841.	3.3	40
58	212-kHz-linewidth, transform-limited pulses from a single-frequency Q-switched fiber laser based on a few-layer Bi ₂ Se ₃ saturable absorber. Photonics Research, 2018, 6, C29.	7.0	29
59	Compact Passive Q-Switching Pr3+-Doped ZBLAN Fiber Laser With Black Phosphorus-Based Saturable Absorber. IEEE Journal of Selected Topics in Quantum Electronics, 2017, 23, 7-12.	2.9	33
60	Tunable and Selectable Multipassband Microwave Photonic Filter Utilizing Reflective and Cascaded Fiber Mach–Zehnder Interferometers. Journal of Lightwave Technology, 2017, 35, 2660-2668.	4.6	15
61	1.61–1.85 \$mu\$m Tunable All-Fiber Raman Soliton Source Using a Phosphor-Doped Fiber Pumped by 1.56 \$mu\$m Dissipative Solitons. IEEE Photonics Journal, 2017, 9, 1-7.	2.0	6
62	Ultra-high Q sphere-like cavities for cascaded stimulated Brillouin lasing. Optics Communications, 2017, 387, 421-425.	2.1	6
63	Chalcogenide glass-on-graphene photonics. Nature Photonics, 2017, 11, 798-805.	31.4	190
64	Mid-infrared integrated photonics on silicon: a perspective. Nanophotonics, 2017, 7, 393-420.	6.0	280
65	CdTe/CdS Quantum Dots: Effective Saturable Absorber for Visible Lasers. IEEE Journal of Selected Topics in Quantum Electronics, 2017, 23, 1-7.	2.9	19
66	Compact visible Q-switching fiber lasers with transition-metal dichalcogenides. , 2017, , .		0
67	Intermode beating mode-locking technique for a rare-earth-doped fiber pulsed laser. Applied Optics, 2017, 56, 6103.	1.8	4
68	12-W average-power, 700-W peak-power, 100-ps dissipative soliton resonance in a compact Er:Yb co-doped double-clad fiber laser. Optics Letters, 2017, 42, 462.	3.3	59
69	716  nm deep-red passively Q-switched Pr:ZBLAN all-fiber laser using a carbon-nanotube saturable absorber. Optics Letters, 2017, 42, 671.	3.3	26
70	Watt-level narrow-linewidth Nd:YAG laser operating on ^4F_3/2→^4I_15/2 transition at 1834 nm. Optics Express, 2016, 24, 3601.	3.4	17
71	Bidirectional operation of 100 fs bound solitons in an ultra-compact mode-locked fiber laser. Optics Express, 2016, 24, 21020.	3.4	33
72	1.63–1.73 µm tunable all-fiber femtosecond pulse generation from a P-doped Raman fiber pumped by 1.56		0

µm dissipative soliton. , 2016, , .

ZHENGQIAN LUO

#	Article	IF	CITATIONS
73	Generation of optical frequency combs in a fiber-ring/microresonator laser system. Optics Letters, 2016, 41, 2576.	3.3	11
74	Passive Q-Switching of a Diode-Pumped Pr:LiYF ₄ Visible Laser Using WS ₂ as Saturable Absorber. IEEE Photonics Journal, 2016, 8, 1-6.	2.0	33
75	Compact diode-pumped continuous-wave and passively Q-switched Nd:GYSO laser at 1.07 µm. Optics and Laser Technology, 2016, 82, 82-86.	4.6	7
76	Compact self-Q-switched green upconversion Er:ZBLAN all-fiber laser operating at 5434  nm. Optics Letters, 2016, 41, 2258.	3.3	23
77	MoS ₂ nano-flake doped polyvinyl alcohol enabling polarized soliton mode-locking of a fiber laser. Journal of Materials Chemistry C, 2016, 4, 9454-9459.	5.5	18
78	Passively <inline-formula> <tex-math notation="LaTeX">\$Q\$ </tex-math> </inline-formula>-Switched Red Pr³⁺-Doped Fiber Laser With Graphene-Oxide Saturable Absorber. IEEE Photonics Technology Letters, 2016, 28, 1755-1758.</inline-formula>	2.5	15
79	Orange-light passively Q-switched Pr^3+-doped all-fiber lasers with transition-metal dichalcogenide saturable absorbers. Optical Materials Express, 2016, 6, 2031.	3.0	42
80	Single- and multi-wavelength Nd:YAlO3 lasers at 1328, 1339 and 1364nm. Optics and Laser Technology, 2016, 81, 1-6.	4.6	14
81	Two-dimensional material-based saturable absorbers: towards compact visible-wavelength all-fiber pulsed lasers. Nanoscale, 2016, 8, 1066-1072.	5.6	246
82	0.1–1-THz High-Repetition-Rate Femtosecond Pulse Generation From Quasi-CW Dual-Pumped All-Fiber Phase-Locked Kerr Combs. IEEE Photonics Journal, 2016, 8, 1-7.	2.0	5
83	Graphene mode-locked and Q-switched 2 - μ m Tm/Ho codoped fiber lasers using 1212-nm high-efficient pumping. Optical Engineering, 2016, 55, 081310.	1.0	16
84	Ultralow-threshold cascaded Brillouin microlaser for tunable microwave generation. Optics Letters, 2015, 40, 4971.	3.3	28
85	Intermode beating mode-locking technique for O-band mixed-cascaded Raman fiber lasers. Optics Letters, 2015, 40, 502.	3.3	14
86	1484-nm two-cascaded Raman fiber laser mode-locked by an intermode-beating mode-locking technique. Optical Engineering, 2015, 54, 046102.	1.0	1
87	Stable, Ultrafast Pulse Mode-Locked by Topological Insulator <inline-formula> <tex-math notation="TeX">\${m Bi}_{2}{m Se}_{3} \$</tex-math </inline-formula> Nanosheets Interacting With Photonic Crystal Fiber: From Anomalous Dispersion to Normal Dispersion. IEEE Photonics Iournal, 2015, 7, 1-8.	2.0	27
88	Topological insulator Bi_2Se_3 based Q-switched Nd:LiYF_4 nanosecond laser at 1313 nm. Optics Express, 2015, 23, 7674.	3.4	76
89	Nonlinear optical absorption of few-layer molybdenum diselenide (MoSe_2) for passively mode-locked soliton fiber laser [Invited]. Photonics Research, 2015, 3, A79.	7.0	227
90	Gold nanoparticles as a saturable absorber for visible 635 nm Q-switched pulse generation. Optics Express, 2015, 23, 24071.	3.4	80

#	Article	IF	CITATIONS
91	635-nm Visible Pr3+-Doped ZBLAN Fiber Lasers Q-Switched by Topological Insulators SAs. IEEE Photonics Technology Letters, 2015, 27, 2379-2382.	2.5	36
92	1212 nm high-efficiently-pumped 2 µm Tm/Ho-co-doped fiber laser Q-switched by graphene. , 2015, , .		0
93	Direct generation of 2  W average-power and 232  nJ picosecond pulses from an ultra-simple Yt double-clad fiber laser. Optics Letters, 2015, 40, 1097. Nanosecond-Pulsed, Dual-Wavelength Passively Q-Switched c-Cut	o-doped	28
94	Nd:YVO <inline-formula><tex-math>\$_{f 4}\$ </tex-math></inline-formula> Laser Using a Few-Layer Bi <inline-formula><tex-math>\$_{f 2}\$</tex-math></inline-formula> Se <inline-formula><tex-math>\$_{f 3}\$</tex-math></inline-formula> Saturable Absorber. IEEE Journal of Selected Topics in	2.9	14
95	Quantum Electronics, 2015, 21, 369-374. 2-D materials-based passively Q-switched 635 nm Pr3+-doped ZBLAN fiber lasers. , 2015, , .		0
96	Passively Q-switched Nd:YAlO_3 nanosecond laser using MoS_2 as saturable absorber. Optics Express, 2014, 22, 28934.	3.4	123
97	Emission properties and CW laser operation of Pr:YLF in the 910 nm spectral range. Optics Express, 2014, 22, 31722.	3.4	21
98	Passively Q-switched linear-cavity erbium-doped fiber laser with few-layer TI: Bi2Se3 saturable absorber. , 2014, , .		4
99	Large-energy, wavelength-tunable, all-fiber passively Q-switched Er:Yb-codoped double-clad fiber laser with mono-layer chemical vapor deposition graphene. Applied Optics, 2014, 53, 4089.	1.8	17
100	2-μm wavelength all-fiber Q-switched double-clad fiber laser using monopiece single-layer chemical-vapor-deposition graphene. Optical Engineering, 2014, 53, 106103.	1.0	3
101	Self-mode-locked 2Âî¼m Tm ³⁺ -doped double-clad fiber laser with a simple linear cavity. Applied Optics, 2014, 53, 892.	1.8	18
102	Low-threshold supercontinuum generation and optimization of PCF-intracavity-excited Q-switched fiber lasers. Optics Communications, 2014, 321, 145-149.	2.1	5
103	Widely-tunable, passively Q-switched erbium-doped fiber laser with few-layer MoS_2 saturable absorber. Optics Express, 2014, 22, 25258.	3.4	183
104	1-, 1.5-, and 2-μm Fiber Lasers Q-Switched by a Broadband Few-Layer MoS ₂ Saturable Absorber. Journal of Lightwave Technology, 2014, 32, 4679-4686.	4.6	318
105	Topological-Insulator Passively Q-Switched Double-Clad Fiber Laser at 2 <formula formulatype="inline"> <tex notation="TeX">\$mu\$</tex>m Wavelength. IEEE Journal of Selected Topics in Quantum Electronics, 2014, 20, 1-8.</formula 	2.9	86
106	Passive Synchronization of 1.06- and 1.53-(mu) m Fiber Lasers Q-switched by a Common Graphene SA. IEEE Photonics Technology Letters, 2014, 26, 1474-1477.	2.5	23
107	Preparation of Few-Layer Bismuth Selenide by Liquid-Phase-Exfoliation and Its Optical Absorption Properties. Scientific Reports, 2014, 4, 4794.	3.3	112
108	High-energy passively Q-switched 2 μm Tm^3+-doped double-clad fiber laser using graphene-oxide-deposited fiber taper. Optics Express, 2013, 21, 204.	3.4	84

#	Article	IF	CITATIONS
109	Numerical modeling of mid-infrared fiber optical parametric oscillator based on the degenerated FWM of tellurite photonic crystal fiber. Applied Optics, 2013, 52, 525.	1.8	20
110	106μm Q-switched ytterbium-doped fiber laser using few-layer topological insulator Bi_2Se_3 as a saturable absorber. Optics Express, 2013, 21, 29516.	3.4	319
111	Diode-pumped Pr^3+:LiYF_4 continuous-wave deep red laser at 698Ânm. Journal of the Optical Society of America B: Optical Physics, 2013, 30, 302.	2.1	58
112	Raman fiber laser harmonically mode-locked by exploiting the intermodal beating of CW multimode pump source. Optics Express, 2012, 20, 19905.	3.4	21
113	Evanescent-Light Deposition of Graphene Onto Tapered Fibers for Passive Q-Switch and Mode-Locker. IEEE Photonics Journal, 2012, 4, 1295-1305.	2.0	118
114	Multiwavelength Dissipative-Soliton Generation in Yb-Fiber Laser Using Graphene-Deposited Fiber-Taper. IEEE Photonics Technology Letters, 2012, 24, 1539-1542.	2.5	56
115	Intermodal-beating mode-locking: toward higher-order harmonic mode-locking of Raman laser. , 2012, ,		0
116	Modeling of mid-infrared fiber optical parametric oscillator. , 2012, , .		0
117	Graphene-Assisted Multiwavelength Erbium-Doped Fiber Ring Laser. IEEE Photonics Technology Letters, 2011, 23, 501-503.	2.5	44
118	Graphene-Induced Nonlinear Four-Wave-Mixing and Its Application to Multiwavelength Q-Switched Rare-Earth-Doped Fiber Lasers. Journal of Lightwave Technology, 2011, 29, 2732-2739.	4.6	70
119	Switchable and tunable multiple-channel erbium-doped fiber laser using graphene-polymer nanocomposite and asymmetric two-stage fiber Sagnac loop filter. Applied Optics, 2011, 50, 2940.	2.1	18
120	Theoretical and Experimental Optimization of O-Band Multiwavelength Mixed-Cascaded Phosphosilicate Raman Fiber Lasers. IEEE Photonics Journal, 2011, 3, 633-643.	2.0	6
121	Continuously wavelength-spacing-tunable and idler-output multiwavelength fiber optical parametric oscillator. Optics Communications, 2011, 284, 2992-2996.	2.1	4
122	Novel L-band multiwavelength Raman fiber laser based on three-stage mixed-cascaded phosphor-silicate Raman process. , 2011, , .		0
123	Spectroscopic analysis of Pr3+:Gd3Ga5O12 crystal as visible laser material. Optical Materials, 2010, 33, 191-195.	3.6	15
124	Graphene-based passively Q-switched dual-wavelength erbium-doped fiber laser. Optics Letters, 2010, 35, 3709.	3.3	461
125	High-performance SOA-based multiwavelength fiber lasers incorporating a novel double-pass waveguide-based MZI. Applied Physics B: Lasers and Optics, 2009, 96, 29-38.	2.2	16
126	Fiber-optic parametric amplifier and oscillator based on intracavity parametric pump technique. Optics Letters, 2009, 34, 214.	3.3	12

#	Article	IF	CITATIONS
127	Multiwavelength Fiber Optical Parametric Oscillator. IEEE Photonics Technology Letters, 2009, 21, 1609-1611.	2.5	21
128	Stable and spacing-adjustable multiwavelength Raman fiber laser based on mixed- cascaded phosphosilicate fiber Raman linear cavity. Optics Letters, 2008, 33, 1602.	3.3	21
129	Multiwavelength Fiber Lasers Based on SOA and Double-pass Mach-Zehnder Interferometer. , 2008, , .		2
130	Theoretical and experimental investigation on backward-pumped Yb ³⁺ -doped double-clad fiber lasers. , 2008, , .		0
131	High power LD-end-pumped Nd:YVO 4 laser as a pump source for Raman fiber laser. , 2007, , .		0
132	Numerical analysis and optimization of optical spectral characteristics of fiber Bragg gratings modulated by a transverse acoustic wave. Applied Optics, 2007, 46, 6959.	2.1	11
133	Analytic modeling of the P-doped cascaded Raman fiber lasers. Optical Fiber Technology, 2007, 13, 22-26.	2.7	5
134	Optimization of the multiwavelength erbium-doped fiber laser in a unidirectional cavity without isolator. Optical Fiber Technology, 2007, 13, 198-201.	2.7	4
135	Simplified analytic solutions and a novel fast algorithm for Yb3+-doped double-clad fiber lasers. Optics Communications, 2007, 277, 118-124.	2.1	21
136	Optimization of dual-wavelength cascaded Raman fiber lasers using an analytic approach. Optics Communications, 2007, 272, 414-419.	2.1	4
137	800mW/1484nm highly efficient two-cascaded phosphosilicate Raman fiber laser pumped by Nd:YVO4 solid-state laser. Optics Communications, 2006, 265, 616-619.	2.1	2